

# THE INFLUENCE OF COOLDOWN CONDITIONS AT TRANSITION TEMPERATURE ON THE QUALITY FACTOR OF NIOBIUM SPUTTERED QUARTER-WAVE RESONATORS FOR HIE-ISOLDE

P. Zhang\*, G. Rosaz, A. Sublet, M. Therasse, W. Venturini Delsolaro  
 CERN, Geneva, Switzerland

## Abstract

Superconducting quarter-wave resonators (QWRs) are to be used in the ongoing linac upgrade of the ISOLDE facility at CERN. The cavities are made of niobium sputtered on copper substrates. They will be operated at 101.28 MHz at 4.5 K providing 6 MV/m accelerating gradient with maximum 10 W power dissipation. In recent measurements, we found the thermal gradient along the cavity during the niobium superconducting transition has an impact on the cavity quality factor. On the other hand, the speed of the cooling down through the superconducting transition turned out to have no influence on the cavity quality factor.

## INTRODUCTION

The High Intensity and Energy (HIE) ISOLDE project is a major upgrade to the current radioactive beam facility at CERN [1, 2]. The main focus is to boost the beam energy from 3 MeV/u to 10 MeV/u for a mass to charge ratio of  $2.5 < A/q < 4.5$ . Superconducting quarter-wave resonators (QWRs) will be used to replace part of the existing normal conducting linac. Each QWR is made of OFE copper (Cu) as a substrate sputtered with thin layers of niobium (Nb). They will provide an accelerating gradient of 6 MV/m on beam axis with a maximum of 10 W power dissipation on the cavity inner surface. A total number of 32 QWRs, 12 low- $\beta$  (6.3%) and 20 high- $\beta$  (10.3%), are planned to be installed to complete the energy upgrade. According to the project schedule, all R&D efforts have been focused on the high- $\beta$  QWR, thus is the focus of this paper. Its main RF parameters are listed in Table 1.

Table 1: The main RF Parameters of the High- $\beta$  QWR.

Parameter	Value
$f_0$ at 4.5 K	101.28 MHz
$\beta_{optimum}$	10.9 %
$E_{peak}/E_{acc}$	5.0
$B_{peak}/E_{acc}$	9.5 mT/(MV/m)
geometry factor $G=R_s Q_0$	30.8 $\Omega$
nominal gradient $E_{acc}$	6 MV/m
max power dissipation at 6 MV/m	10 W
$Q_0$ at $E_{acc}=6$ MV/m	$4.7 \times 10^8$

The influence of cooldown conditions on the cavity performance has become a hot topic in SRF community in

\*pei.zhang@cern.ch

recent years. Many labs have done dedicated experimental studies mainly on bulk Nb cavities and several theories have been developed aiming to explain the results in terms of thermal current induced flux trapping and the efficiency of flux expulsion due to cooldown dynamics. These can be referred to [3–5]. In this paper, we present our experimental studies on cooldown conditions in Nb-sputtered-on-copper quarter-wave resonators.

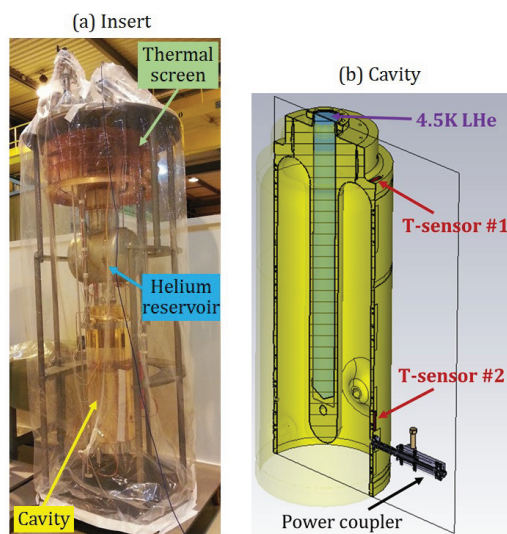


Figure 1: The insert for the vertical test at 4.5 K and the cavity geometry with temperature sensors.

After frequency tuning, substrate surface treatment and Nb sputtering [6, 7], all QWRs are tested in the vertical cryostat at 4.5 K at CERN before assembling into the cryomodule. The insert for the vertical test is shown in Fig. 1(a) [8]. The liquid helium (LHe) is delivered to the cryostat where its level is kept constant in the reservoir. The cavity inner conductor is hollow and filled with LHe from the reservoir as shown in Fig. 1(b). The rest of the cavity is cooled by conduction. During the cooldown process, a temperature gradient can be built up along the cavity with the bottom of the outer conductor is warmer than the top part. Temperature sensors (T-sensors) are mounted on the cavity outer wall at various locations and two of them, one on the top and the other close to the bottom as shown in Fig. 1(b), are used for the following study to characterize the thermal gradient and the cooldown speed. The quality factor ( $Q_0$ ) at different accelerating gradient in the cavity

was measured at 4.5 K for each cavity. The dependence of cavity surface resistance on the thermal gradient and the cooldown speed is characterized and presented in the following sections.

## THE DEFINITION OF THERMAL GRADIENT AND THE FITTING OF SURFACE RESISTANCE

During the cooldown process, the cavity temperature is being constantly monitored. The readings of the two T-sensors shown in Fig. 1(b) during initial cooldown from room temperature is shown in Fig. 2(a) of one example cavity. The thermal gradient  $\Delta T$  along the cavity at any time may be defined as the temperature difference between the two T-sensors as

$$\Delta T = T_2 - T_1. \quad (1)$$

This is shown in Fig. 2(b). The thermal gradient during normal conducting (NC) to superconducting (SC) transition,  $\Delta T_{NC \rightarrow SC}$ , is of particular interest and is defined as the average  $\Delta T$  within the range of  $\pm 1$  K from the critical temperature 9.5 K read from T-sensor #2. This is depicted as the filled area in green in Fig. 2(a). The standard deviation from the average value within the same temperature range may be defined as the uncertainty of  $\Delta T_{NC \rightarrow SC}$ . By this definition, the thermal gradient during transition shown in Fig. 2 is calculated to be  $0.42 \pm 0.09$  K.

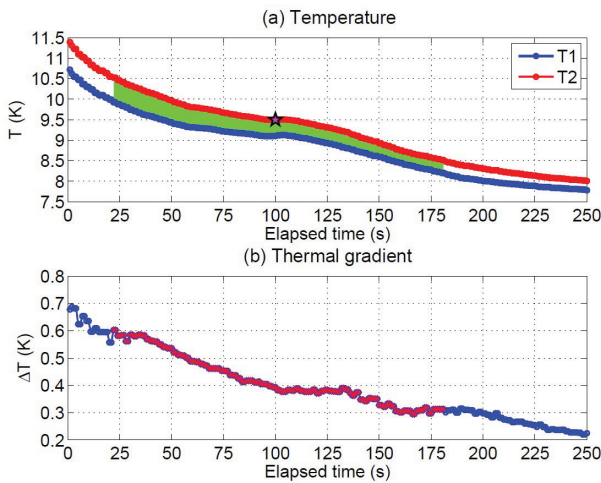


Figure 2: Temperature reading and thermal gradient vs. time during an initial cooldown from the room temperature.

The surface resistance  $R_s$  can be derived from the measured cavity  $Q_0$  by [9]

$$R_s = \frac{G}{Q_0} = \frac{30.8 \Omega}{Q_0}, \quad (2)$$

where  $G$  is the cavity geometry factor as listed in Table 1. This is shown in Fig. 3 as the dots. The surface resistance

ISBN 978-3-95450-178-6

at low field may be fitted in a linear manner as

$$R_s = R_{s0} + R_{s1} \cdot E_{acc}, \quad (3)$$

where  $R_{s0}$  is the zero-field surface resistance and  $R_{s1}$  is the linear slope of the surface resistance with regarding to the accelerating field  $E_{acc}$ . Fig. 3 shows one example of the fitting where the fitting range is from 0 to 3.5 MV/m of  $E_{acc}$ . The uncertainties for  $R_{s0}$  and  $R_{s1}$  may be defined as the 95% confidence level derived from the fitting. This is indicated by the dash lines around the fitting in Fig. 3. The  $R_s$  possesses good linearity at low  $E_{acc}$ .

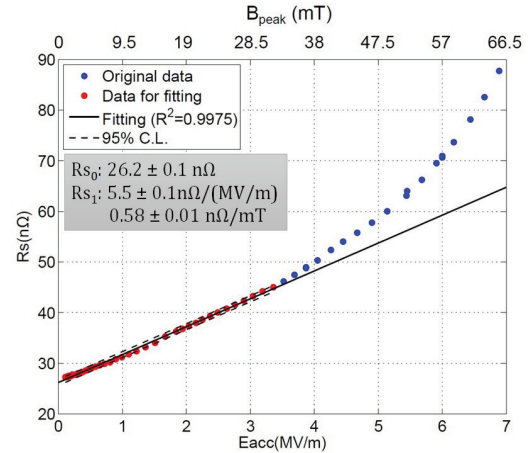


Figure 3: The linear fitting of the surface resistance.

During the RF cold test of each cavity, thermal cyclings (T-cycles) are usually performed after the initial cooldown to 4.5 K from room temperature. These are conducted by warming up the cavity to 12-20 K, well above the critical temperature of 9.5 K, and cooldown again to 4.5 K. The diverse cooldown processes during T-cycles produce a variety of thermal gradients and cooldown speeds. The linear components of the surface resistance,  $R_{s0}$  and  $R_{s1}$ , are obtained for each cavity by fitting Eq. 3. The fitting  $E_{acc}$  stops where the  $R_s$  starts to deviate from the linear behaviour as shown in red in Fig. 3. Depending on individual cavity performance, the fitting range is not necessarily the same for each cavity. The fitted  $R_{s0}$  and  $R_{s1}$  of each cavity is shown in Fig. 4 with regarding to the thermal gradient presented during the related cooldown process. The surface resistance has an evident dependence on the cavity thermal gradient, where large  $\Delta T_{NC \rightarrow SC}$  leads to high  $R_s$ . All cavities shown in Fig. 4 were Nb sputtered with the same baseline coating ‘‘recipe’’ [7].

## THE IMPACT OF THERMAL GRADIENT ON SURFACE RESISTANCE

The dependences of  $R_{s0}$  and  $R_{s1}$  on  $\Delta T_{NC \rightarrow SC}$  are not the same for all cavities. The  $R_s$  of QP-series and some QS cavities have lower sensitivities to thermal gradient, where QS2.1 and QS3.1 possess higher sensitivities

SRF Technology - Cavity

E07-Non-Elliptical performance

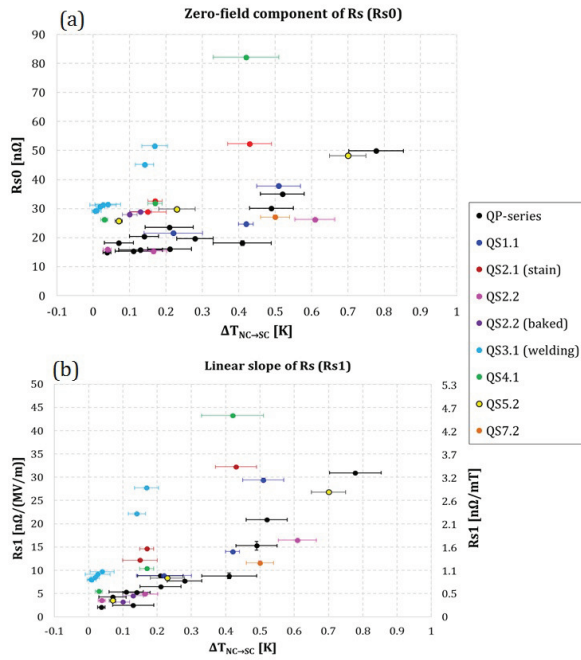


Figure 4: The dependence of fitted  $R_{s0}$  and  $R_{s1}$  on thermal gradient.

(steeper slope). For all cavities, a large thermal gradient was often observed during the initial cooldown from room temperature due to the cooling scheme (Fig. 1) and the massive weight of the cavity ( $\sim 180$  kg). Thus the cavity surface resistance is always larger at the initial cooldown. The cavity performance can be improved by T-cycles to  $\sim 15$  K where the thermal gradient is minimized. This has been studied for bulk Nb cavities [3].

### QS2 (Substrate Surface Defect, Low- $T$ Bake)

The first coating of the cavity, QS2.1, does not have ideal  $R_{s0}$  or  $R_{s1}$  as shown in Fig. 5. After minimizing  $\Delta T_{NC \rightarrow SC}$  down to 0.15 K, the zero-field  $R_s$  is still about 30 n $\Omega$ , which doubles the best value seen on other cavities. This is also true for  $R_{s1}$ . In addition, the sensitivity of both  $R_{s0}$  and  $R_{s1}$  to thermal gradient is higher than QP cavities. This might link to the surface quality of the Cu substrate before coating. A stain of a few mm was observed at the top part of the cavity. Then a heavy chemical etching was conducted and the stain was not visible anymore before coating. However the impact might still exist due to the location of the stain sees high RF magnetic field [10].

Then the Nb film was stripped and the substrate was sputtered with Nb again by the same “recipe”. The performance is shown in Fig. 5 as QS2.2. Both  $R_{s0}$  and  $R_{s1}$  are largely minimized and a  $R_{s0}$  of 15 n $\Omega$  corresponding to a  $Q_0$  of  $2 \times 10^9$  was achieved. The sensitivities to thermal gradient are now in line with QP cavities. Due to the onset of field emission at high-field region, an additional rinsing [6] of the cavity was conducted. Then the cavity was baked for a longer time at  $\sim 67^\circ\text{C}$  than usual due

SRF Technology - Cavity

E07-Non-Elliptical performance

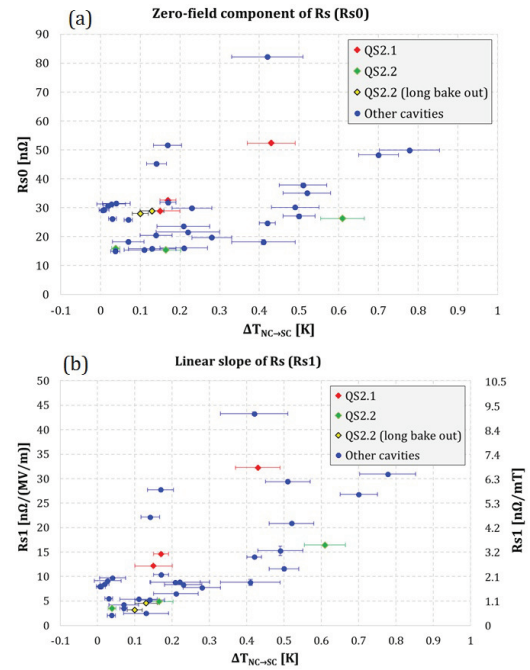


Figure 5: The dependence of fitted  $R_{s0}$  and  $R_{s1}$  on thermal gradient with cavity QS2.1 and QS2.2 highlighted.

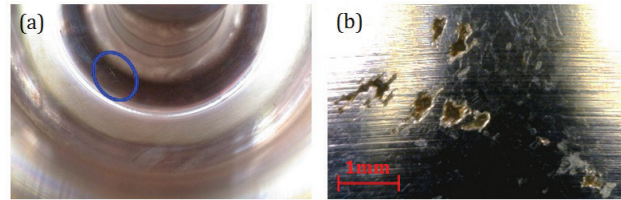


Figure 6: The stain on the inner surface of the copper substrate QS2.1 before chemical etching.

to technical reasons as shown in Table. 2. This long low-temperature bakeout boosts  $R_{s0}$  back to the original value of QS2.1 although  $R_{s1}$  was intact from the first test.

Table 2: The Bakeout Time of QS2.2.

	Duration when $T > 67^\circ\text{C}$	$T_{\text{max}}$
1 <sup>st</sup> test	13.2 hours	$69^\circ\text{C}$
2 <sup>nd</sup> test	26.7 hours	$75^\circ\text{C}$

### QS3 (Substrate Surface Defect, Repairing Weld)

Compared with other cavities, QS3.1 has the largest sensitivity of both  $R_{s0}$  and  $R_{s1}$  to the thermal gradient as shown in Fig. 4. This may link to the E-beam welding of the substrate on the cavity top part. A crack was observed after the chemical etching as shown in Fig. 7(a). Two additional weldings were subsequently done at CERN in order to cover the crack thus repairing the substrate as shown in Fig. 7(b). The additional weldings might ease the magnetic flux trapping, therefore an already small thermal gradient

ISBN 978-3-95450-178-6

767

can still lead to high  $R_{s0}$  and  $R_{s1}$  together with the highest sensitivity to  $\Delta T_{NC \rightarrow SC}$  among all tested cavities.

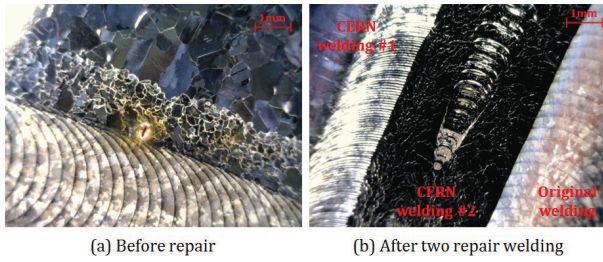


Figure 7: (a) The feature observed on the inner surface of copper substrate QS3.1 after final chemical etching & smoothing. (b) The two repairing welding to cover the feature.

QS7 (High Bias Coating)

QS7.1 was sputtered with a modified cathode biased at -120 V, while the baseline “recipe” uses a standard cathode biased at -80 V. The high-bias voltage increases the ion bombardment on the Nb film, thus causes higher stress on the Nb layer. After coating, delaminations were observed on the coated sample located on the top part of the cavity as shown in Fig. 8. However the Nb film looks denser than that coated with baseline “recipe” [11]. Fig. 9 shows the surface resistance as a function of  $E_{acc}$ . An evidently large slope at low-field can be seen. Relating to thermal gradient,  $R_{s0}$  follows the same trend as other cavities although a much larger and sensitive  $R_{s1}$  was observed as shown in Fig. 10. The cavity was subsequently stripped and re-coated with the standard “recipe” (QS7.2). Both  $R_{s0}$  and  $R_{s1}$  are then largely reduced to the level of QP cavities.

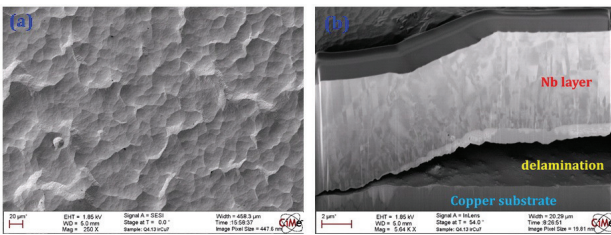


Figure 8: The SEM-FIB cross section pictures of a sample on the inner conductor at cavity top part. The coating was done by a modified cathode with -120 V DC bias voltage [12, 13]. (Courtesy B. Bartova from EPFL-CIME)

THE IMPACT OF COOLDOWN SPEED ON SURFACE RESISTANCE

The cooldown speed of a cavity going through SC transition may be defined as how fast the temperature of cavity bottom (T-sensor #2) decreases from 10.5 K to 8.5 K and its unit is mK/s. By this definition, it takes 159 seconds for the cavity shown in Fig. 2 to complete the change

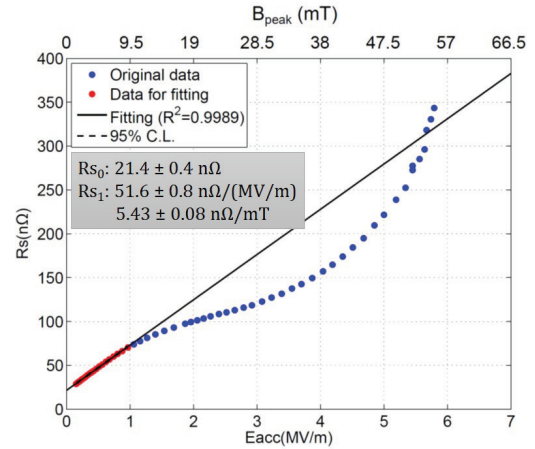


Figure 9: The linear fitting of the surface resistance of QS7.1.

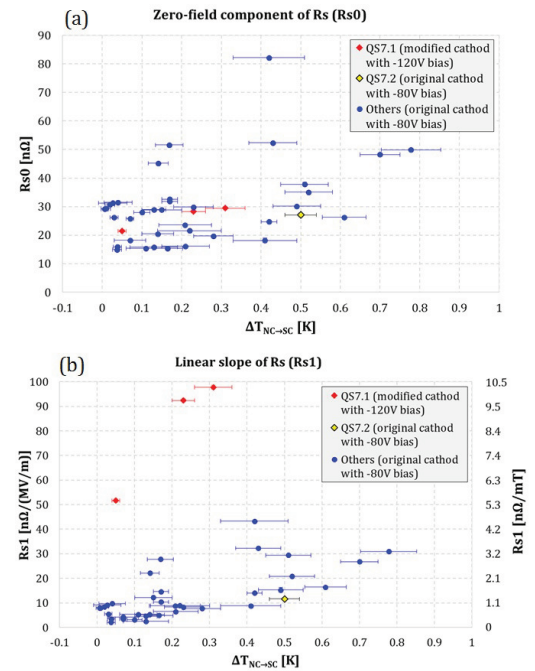


Figure 10: The dependence of fitted  $R_{s0}$  and  $R_{s1}$  on thermal gradient with cavity QS7.1 and QS7.2 highlighted.

(the filled area in green) and thus the cooldown speed is calculated to be 12.6 mK/s. The thermal gradient versus the cooldown speed is plotted in Fig. 11 for various cavities. The initial cooldown of the cavity from room temperature usually produces a large thermal gradient and slow cooldown rate, while small thermal gradients with a large spread of cooldown speeds are presented in T-cycles.

In order to see only the impact of cooldown speed, the thermal gradients have been categorized into four groups:  $0.46 \pm 0.08$  K,  $0.20 \pm 0.04$  K,  $0.12 \pm 0.02$  K and  $0.05 \pm 0.03$  K. Within each temperature group, a spread of cooldown speeds can still be observed. The dependence of  $R_{s0}$  and  $R_{s1}$  on the cooldown speed is shown in Fig. 12.

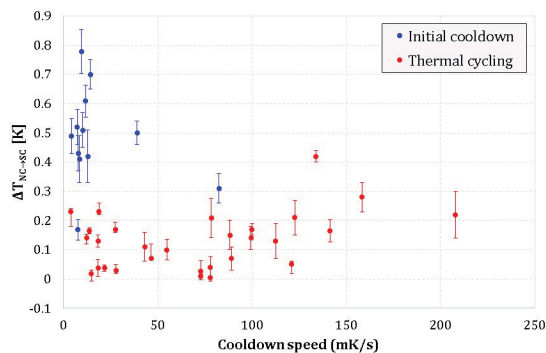


Figure 11: The dependence of thermal gradient on the cooldown speed.

No obvious link between  $R_s$  and cooldown rate can be observed in any temperature category. In general, QP cavities outperform QS cavities in each temperature category. The spread of  $R_{s0}$  and  $R_{s1}$  with a cooldown speed below 20 mK/s are due to the spread of performance among different cavities.

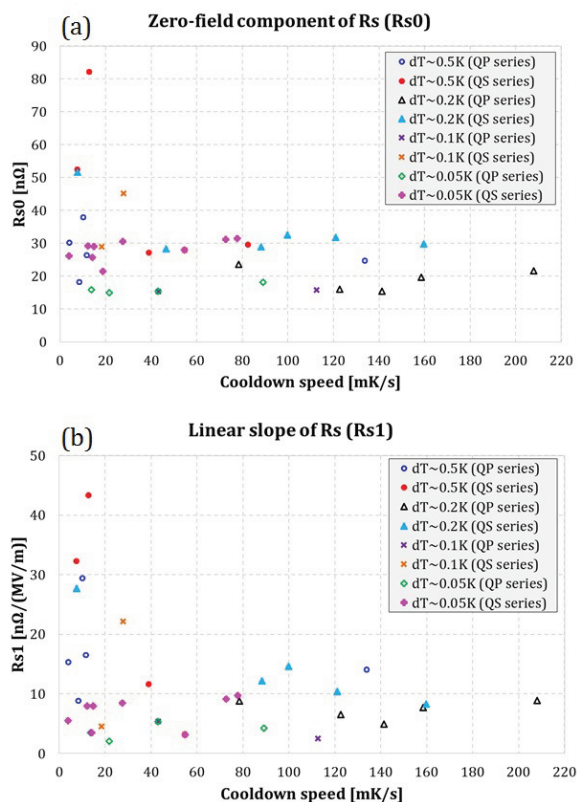


Figure 12: The dependence of fitted  $R_{s0}$  and  $R_{s1}$  on cooldown speed.

### FINAL REMARKS

For HIE-ISOLDE Nb-sputtered quarter-wave resonators, a thermal gradient can be built up along the cavity during the superconducting transition. The low-field cavity

surface resistance can be fitted into zero-field component ( $R_{s0}$ ) and linear slope ( $R_{s1}$ ). In the cavity vertical tests, we observed a direct impact of thermal gradient on both  $R_{s0}$  and  $R_{s1}$ . This might be due to trapped magnetic flux induced by thermal currents. This study is still ongoing. On the other hand, the cavity performance does not depend on how fast the cavity is being cooled through the superconducting transition.

### ACKNOWLEDGEMENTS

We thank S. Bizzaglia, S. Fiotakis, M. Gourragne, G. Pechaud and G. Fernandez at CERN for their excellent technical support. We are grateful to S. Aull and T. Junginger for very enlightening discussions. This work has been supported partly by a Marie Curie Early Initial Training Network Fellowship of the European Community's 7th Programme under contract number PITN-GA-2010-264330-CATHI.

### REFERENCES

- [1] W. Venturini Delsolaro *et al.*, "Status of the HIE Isolde Project including Cryomodule Commissioning," *these proceedings*, TUBA01, SRF2015, Whistler, Canada, (2015).
- [2] M. Therasse *et al.*, "First Phase HIE-ISOLDE Cryomodules Assembly at CERN," *these proceedings*, TUPB106, SRF2015, Whistler, Canada, (2015).
- [3] O. Kugeler *et al.*, SRF2009-TUPPO053, <http://jacow.org/>
- [4] J.-M. Vogt *et al.*, *Phys. Rev. ST Accel. Beams* 16, 102002 (2013).
- [5] A. Romanenko *et al.*, *J. Appl. Phys.* 115, 184903 (2014).
- [6] M. Therasse *et al.*, "Series Superconducting Cavity Production for the HIE-ISOLDE Project at CERN," in *Proceedings of LINAC2014*, 2014.
- [7] A. Sublet *et al.*, IPAC2014-WEPRI042, <http://jacow.org/>
- [8] O. Capatina *et al.*, IPAC2011-MOPC103, <http://jacow.org/>
- [9] H. Padamsee, J. Knobloch and T. Hays, *RF superconductivity for accelerators*. Wiley-VCH, second ed., 2008.
- [10] P. Zhang *et al.*, "The multipacting study of niobium sputtered high-beta quarter-wave resonators for HIE-ISOLDE," *these proceedings*, TUPB076, SRF2015, Whistler, Canada, (2015).
- [11] A. Sublet *et al.*, IPAC2015-WEPHA021, <http://jacow.org/>
- [12] B. Bartova *et al.*, IPAC2015-WEPHA022. <http://jacow.org/>
- [13] A. Sublet *et al.*, "Developments on SRF Coatings at CERN," *these proceedings*, TUPB027, SRF2015, Whistler, Canada, (2015).